RANDOMNESS-BASED INTEGRATION OF MULTI-VIEWPOINT IMAGERY FOR *AS-IS* ROADWAY MODEL GENERATION

Kohji Kamejima

Faculty of Information Science and Technology, Osaka Institute of Technology
1-79-1 Kitayama, Hirakata 573-0196 JAPAN
phone: +81(Japan)-72-866-5406, fax: +81(Japan)-72-866-8499, email: kamejima@is.oit.ac.jp
web: http://www.is.oit.ac.jp/~kamejima

ABSTRACT

A new framework is presented for identifying roadway pattern in multi-viewpoint imagery. By applying fractal sampling to scene and satellite imagery, chromatic complexity of random texture is extracted and adapted for multi-viewpoint association. The feasibility of the framework is investigated through experimental studies.

1 Introductory Remarks

Computational resources combined with advanced vehicle mechanisms rapidly expands the scope of 'informatic vicinity [7] in which machine perception is delegated and networked to support human's situation understanding and decision making. For instance, students knowledge can be expanded interactively by space craft to be operated from classroom [3]. Final decision for social safety in large scale natural disaster is missioned to the governorship of information gathering and damage evaluation systems [5]. The mobility of computer controlled vehicles, in particular, exceeds by far human's inherent maneuverability for information gathering and situation understanding [11]. As a consequence of evolution in uproarious illumination and reflection [12], the range of human's perception is restricted to physical perspective from a specific view point. For on-going conformability of such human centered systems, thus, perceptive delegation is required to maintain direct access to *as-is* surroundings under the schematics of serious contradiction: subsequent maneuvering processes is anticipatively adapted to unstructured scene. To make allowance for human's decision, the informatic vicinity should be supervenient to entire the real world.

Supported by the imagination of a bird's eye view, the maneuverability of vehicles is substantiated within multi-aspect representation of scenes: two dimensional description of local terrain and a sequence of 2.5D perspectives. This implies that autonomous maneuvering processes guided by human and/or machine intelligence maintain their own integrity within vehicles specific internal world to be generated as dynamic link of the two-aspect representations. The integrity of maneuvering systems makes it possible to open a human access pass to planning process on *as-is* map [13]. as well as simultaneous mapping-navigation process based on *in-situ* scene images [2]. To develop the human access pass to integrated planning-mapping-navigation scheme, however, the comprehensiveness of the scene should be restored within the vehicles beyond aspect specific processes.

Three decades of investigations in cognitive science have revealed that humans are endowed with *a priori* concept of space to integrate multiple aspects of the world into terrain-perspective structure. Despite the inaccessibility to human's inherent concept of space, the terrain-perspective integration process has been simulated on satellite-roadway-vehicle network [8] where the expansion of a roadway area is identified with the support of scale-chromatic randomness. By invoking the robustness of the randomness distribution, the entire sequence of scene images can be associated with a maneuvering plan along a roadway pattern in a satellite image.

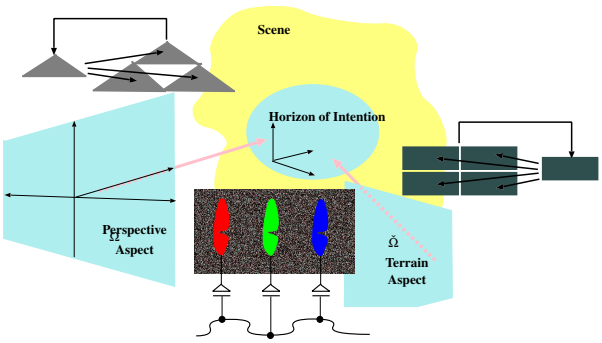

Figure 1: Multi-Aspect Approach to Complex Scene

On this terrain-perspective structure, two types of prediction are implemented as essential part of for autonomous road following mechanism: successive extension of roadway pattern in a satellite image and one step prediction of the scene to be encountered. For stable operation, the vehicle control systems require geometric description of the roadway in the predicted scene. In this paper, we consider terrain-perspective association mechanism for *as-is* roadway model generation.

2 Randomness-based Approach

Despite the diversity of the terrain and the discrepancy of imaging conditions, we can exploit the randomness covering natural objects as a robust feature for associating multi-viewpoint imagery [6] [9]. In this section, preliminary results of randomness based approach are summarized.

Following the collage theorem within the context of multi-fractal modeling [1], the expansion of the open space in a bird's eye view and scene perspectives can commonly be identified with the same class of fractal attractor Ξ satisfying

$$\Xi = \bigcup_{\mu_i \in \nu} \mu_i(\Xi), \qquad (1)$$

with a fixed set of contraction mappings $\nu = \{\mu_i\}$ as illustrated in Fig. 1. In this figure, a roadway segment in the satellite image is modeled by Sierpinski's 'carpet' generated in the terrain aspect $\breve{\Omega}$ by using the following mapping set

$$\breve{\nu} \ni \breve{\mu}_i : \qquad \breve{\mu}_i(\breve{\omega}) = \frac{1}{2}\left(\breve{\omega} + \breve{\omega}^f_{\breve{\mu}_i}\right), \qquad p_{\breve{\mu}_i} = \frac{1}{4}, \quad (2)$$

where $\breve{\omega} \in \breve{\Omega}$ denotes a pixel in the satellite image and $\omega^f_{\mu_i}$ denotes the vertices of the carpet. This segment is mapped from the satellite image to associated scene images to yield a skewed attractor called Sierpinski's 'gasket' via the self-similarity process (1) with

$$\nu \ni \mu_i : \qquad \mu_i(\omega) = \frac{1}{2}\left(\omega + \omega^f_{\mu_i}\right), \qquad p_{\mu_i} = \frac{1}{3}, \quad (3)$$

in the perspective aspect $\Omega = \{\omega\}$. In Eq. (3), $\omega^f_{\mu_i}, i = 1,2,3$ are specified in terms of the vanishing point and the width of the roadway area in the scene image. Noticing that an attractor point $\xi \in \Xi$ can be mapped finally to entire pattern Ξ through random selection of $\mu_i \in \nu$, i.e.,

$$\xi_{t+1} \quad = \quad \mu_i(\xi_t), \quad (4)$$

the density of reachable points ξ_∞ can be visualized as a distribution $\chi^{\mathfrak{p}}_\Xi$ invariant under the self-similarity process (1).

Following multi-scale approach [10], [4], let $\hat{\sigma}_\omega$ be the estimate of scale information induced by the invariant measure $\chi^{\mathfrak{p}}_\Xi$ in the scene image Ω. The variation of the scale information is bounded by the following pixel wise evaluation

$$\hat{\sigma}_\omega \quad = \quad \sqrt{2 f_\omega / |\Delta f_\omega|}, \quad (5)$$

where f_ω denotes the brightness distribution in the scene image. Through the perspective projection, randomness distribution in the carpet is observed in terms of the linear scale shift towards the vanishing point in the gasket. Hence we have the following estimate

$$\hat{\chi}^{\mathfrak{p}}_\Xi \quad = \quad \frac{1}{\sqrt{2\pi\bar{\sigma}_d^2}} \exp\left[-\frac{|\hat{\sigma}_\omega - \bar{\sigma}_d|^2}{2\bar{\sigma}_d^2}\right], \quad (6a)$$

of the perspective projection:

$$\bar{\sigma}_d \quad = \quad \frac{\sigma_0}{d_\infty - d_0}(d_\infty - d). \quad (6b)$$

In Eq. (6), σ_0 denotes the maximal scale of the noise component and d designates the depth parameter indexed along the direction of the roadway. In many practical scene, the maximal scale can be estimated by $\sigma_0 = 2 \cdot \hat{\sigma}_{\min}$, where $\sigma_{\min}$ denotes the minimal value of the estimate $\hat{\sigma}$ in the image plane.

Based on the 'noisy' observation $\hat{\chi}^{\mathfrak{p}}_\Xi$, the expansion of the roadway under the self-similarity condition (1) is indexed in terms of the solution to the following equation:

$$\frac{1}{2}\Delta\varphi(\omega|\nu) + \rho[\hat{\chi}^{\mathfrak{p}}_\Xi - \varphi(\omega|\nu)] \quad = \quad 0, \quad (7)$$

where $\rho = \log_2 \|\nu\|$. By using the conditional probability (7), the consistency of the mapping set ν is verified through the detection of finite invariant subset:

$$\Theta \quad = \quad \left\{\theta \in \tilde{\Theta} \;\middle|\; \exists \mu_i \in \nu : \mu_i^{-1}(\theta) \in \Theta\right\}, \quad (8)$$

Figure 2: Cooperative Decision in Informatic Vicinity

where $\tilde{\Theta}$ is the local maxima of $\varphi(\omega|\nu)$.

Let $f^{\mathrm{RGB}}_\omega = [\mathrm{R}_\omega \quad \mathrm{G}_\omega \quad \mathrm{B}_\omega]^T$ be the intensity vector of three primaries and define $\phi_\omega = f_\omega / \left|f^{\mathrm{RGB}}_\omega\right|$. By applying stochastic dynamics (4) to observed scene image, we have the following 'palette' as a representation for the chromatic complexity of roadway area in the scene image:

$$\mathfrak{s} \quad = \quad \left\{\phi_\xi \;\middle|\; \xi \in \Xi\right\}. \quad (9)$$

The palette $\breve{\mathfrak{s}}$ is extracted in the satellite image and matched with $\mathfrak{s}$ to adjust the location of the roadway segment in the satellite image. Due to the robustness of the palette representation, the roadway segment can be extended *prior to* physical arrival as shown in Fig. 2; the palette $\mathfrak{s}$ was sampled within the lane of start point with the scene image (lower left sub-window); $\mathfrak{s}$ was matched with the palette $\breve{\mathfrak{s}}$ extracted on associated segment in the satellite image to extend the roadway pattern; the extended roadway pattern reached a destination of the satellite image *prior to* physical arrival to the scene (upper left sub-window). Such an anticipative road following process provides initial guess of the depth and the width of the roadway pattern in the scene image.

3 Fractal Coding of Open Space

Let $\vec{\Omega}^d$ be the vector towards the vanishing point in the scene image and consider the projection of the roadway segments detected *a priori* in the bird's eye view into scene image. By identifying the fixed points $\Omega^f = \left\{\omega^f_{\mu_i}\right\}$ in terms of the depth and width of the roadway pattern, the scene image can be partitioned into the following regions

$$\Lambda_i : \left\{\omega \in \Omega \;\middle|\; |\omega - \omega^f_{\mu_i}| < |\omega - \omega^f_{\mu_j}|, \quad \text{for } \omega^f_{\mu_j} \neq \omega^f_{\mu_i}\right\},$$

with statistical moments $(\bar{\omega}_i, \Sigma_i)$ conditioned by ν:

$$\int_{\Lambda_i} (\omega - \bar{\omega}_i)\varphi(\omega|\nu)dP(\omega) = 0,$$

$$\Sigma_i \quad = \quad C_i \int_{\Lambda_i} (\omega - \bar{\omega}_i)(\omega - \bar{\omega}_i)^T \varphi(\omega|\nu)dP(\omega),$$

where C_i denotes normalization constant. In this partitioning, the expansion of the domains Λ_i is indexed in terms of the following 'Laplacian-Gaussian basin':

$$\Lambda_i^{\mathfrak{G}} = \left\{ \lambda \in \Lambda_i \;\middle|\; \left(\frac{1}{2} \varepsilon_\lambda^T \Sigma_i^{-1} \varepsilon_\lambda - 1 \right) < 0 \right\}, \tag{10}$$

where $\varepsilon_\lambda = \lambda - \bar{\omega}_i$. To each basin $\Lambda_i^{\mathfrak{G}}$, we have the following circumscribing polygon

$$\left(\vec{\Omega}_{ij}^f \right)^T R(\pi/2) \left(\partial_\omega - \omega_{\mu_j}^f \right) = 0, \tag{11a}$$

$$\left(\vec{\Omega}_j^\partial \right)^T R(\pi/2) \left(\partial_\omega - \bar{\omega}_j \right) = 0, \tag{11b}$$

where ∂_ω is the contact point with $\Lambda_i^{\mathfrak{G}}$; $\vec{\Omega}_{ij}^f$ and $\vec{\Omega}_j^\partial$ are unit vector associating the fixed point $\omega_{\mu_j}^f$ with $\omega_{\mu_i}^f$ and $\bar{\omega}_j$, respectively; R denotes 2D rotation matrix. By adjusting ∂_ω to the boundary of the Laplacian-Gaussian basin (10) along external normal vector $\vec{\Omega}_{ij}^\perp$, we have the following adaptation scheme of the fixed point Ω^f:

$$\begin{aligned} d\omega_{\mu_j}^f &= -\kappa \psi_j (\omega_{\mu_j}^f - \bar{\omega}_j), \\ \psi_j &= \frac{1}{2} (\partial_\omega - \bar{\omega}_j)^T \Sigma_j^{-1} (\partial_\omega - \bar{\omega}_j) - 1, \\ & \partial_\omega - \bar{\omega}_j = -Q_j^{-1} K_{ij} \left(\omega_{\mu_j}^f - \bar{\omega}_j \right), \\ & Q_j = \left(\vec{\Omega}_{ij}^\perp \right)^T \Sigma_j \left(\vec{\Omega}_{ij}^\perp \right), \\ & K_{ij} = \Sigma_j \left(\vec{\Omega}_{ij}^\perp \right) \left(\vec{\Omega}_{ij}^\perp \right)^T. \end{aligned} \tag{12}$$

In this scheme, the fixed points $\left\{ \omega_{\mu_j}^f \right\}$ are mutually separated by the expansion of the Laplacian-Gaussian basins (10); on the other hand, the expansion of fractal attractor to be generated by confined in terms of the contact points $\{ \partial\omega \}$. As the result of this antagonistic dynamics, the update $d\omega_{\mu_i}^f$ are coordinated via the integration rule:

$$\sum_j |\psi_j| \quad \rightarrow \quad \min. \tag{13}$$

Let the fixed points $\omega_{\mu_i}^f$ in Eq. (3) be adjusted following Eqs. (10) and (12). Then the mapping set ν generates the fractal attractor covering a part of the open space satisfying the scale space model (6) directed to $\vec{\Omega}^d$; the projection of the roadway segment. The consistency of the attractor with the distribution of the randomness is verified via the computational test (8); the existence of invariant features Θ implies that the range of designed imaging process (4) generates a version of fractal attractor Ξ covering a part of roadway area. Thus, the direction $\vec{\Omega}^d$ of extended segment in the satellite image provides sufficient information to induce a fractal code of an open space with *as-is* visualization in observed scene.

4 Fractal Boundary Adaptation

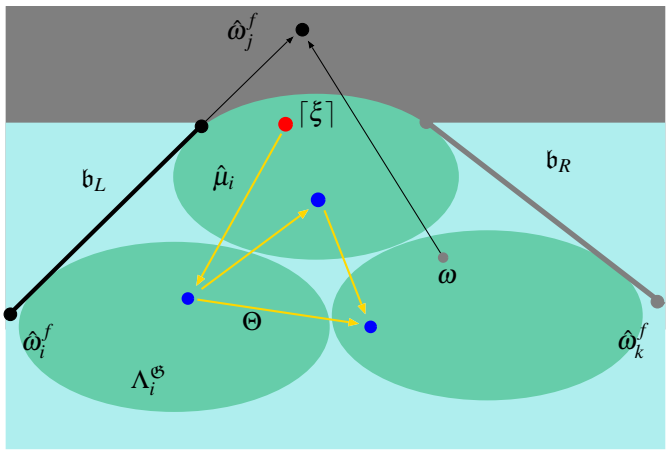

Figure 3: Fractal Coding of Laplacian-Gaussian Basin

By the robustness of scale-chromatic randomness, we can match roadway segments to be extended in the satellite image with encountered scene self-reflectively; a pixel in a Laplacian-Gaussian basin ω is randomly attracted to one of fixed points in Ω^f via the generativity of the self-similarity process; despite such a nondeterministic allocation, the structural consistency of the set Ω^f is verified by the existence of the capturing probability $\varphi(\omega|\nu)$ supporting invariant subset Θ in the local maxima $\tilde{\Theta}$. In many practical scenes, however, the maneuverable area should be confined by various objects and/or sign patterns distributed in the roadway pattern. Despite the self-reflectivity on discrete features $\tilde{\Theta}$, the fractal code ν spans the open space over obstacle images at which the scale space representation (6) breaks down. To apply the fractal code to the control of vehicle mechanisms, hence, the fixed points $\Omega^f = \left\{ \omega_{\mu_i}^f \right\}$ should be adapted for all the attractor points ξ_t to be located in an obstacle-free sub-region.

To this end, left and right boundaries of the open space model is defined in terms of the mapping set $\nu = \{ \mu_i \}$ and relocated to avoid the obstacle objects and/or sign patterns as illustrated in Fig. 3 where $\omega_{\mu_j}^f$ and $\omega_{\mu_i}^f$ ($\omega_{\mu_k}^f$) denote the vanishing point and left (right) boundary point, respectively. It should be noted that the fractal attractor is identified with the totality of the fixed points associated with all finite chains of the contraction mappings. Noting this, in this figure, the left and right boundaries, $\mathfrak{b}_L$ and $\mathfrak{b}_R$, are generated as the fractal attractors associated with the mapping sets $\nu_{\mathfrak{b}}^L$ and $\nu_{\mathfrak{b}}^R$ given by

$$\mathfrak{b}_L : \quad \nu_{\mathfrak{b}}^L = \{ \mu_j, \mu_i \} \tag{14a}$$

$$\mathfrak{b}_R : \quad \nu_{\mathfrak{b}}^R = \{ \mu_j, \mu_k \} \tag{14b}$$

respectively. In Fig. 3, $\lceil \xi \rceil$ denotes the nearest point to the fixed point ω_{μ_j} in the invariant subset Θ. By using the point $\lceil \xi \rceil$, we can specify the horizon of the stochastic-computational verification as well as depth of the boundary information $(\mathfrak{b}_L, \mathfrak{b}_R)$ to be marked in the scene image.

Suppose that the break down pixels of the scale space model (6) is detected as the boundary in the scene image and consider the road relocation process: match the fixed points $\Omega^f = \left\{ \omega_{\mu_i}^f \right\}$ with the boundary image of open space to adapt

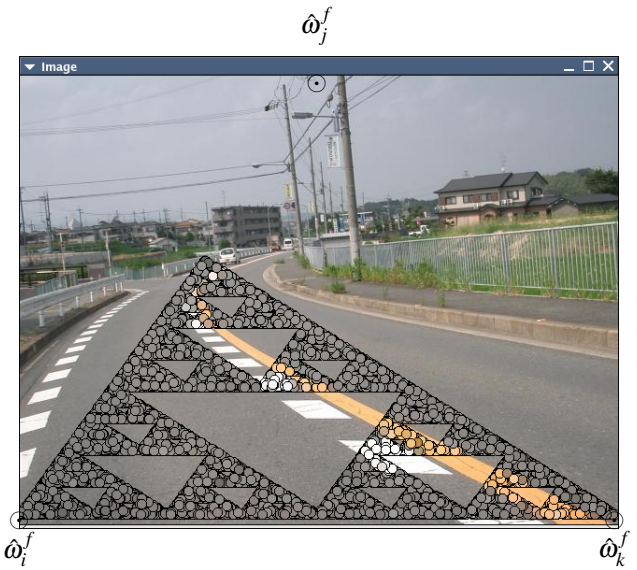

Figure 4: Fractal Coding

the fractal code ν. Since the boundary image $\mathfrak{b}_L$ ($\mathfrak{b}_R$) is generated via the following nondeterministic dynamics

$$\hat{\xi}_{t+1} = \mu_t(\hat{\xi}_t), \qquad \mu_t \in \nu^L_{\mathfrak{b}_L}(\nu^R_{\mathfrak{b}_L}) \tag{15}$$

we have the following update scheme for the fixed points:

$$d\omega^f_{\mu_j} = \gamma \sum_{\mu_j \in \nu} \hat{\psi}(\hat{\xi}_t|\mu_j), \tag{16a}$$

$$\hat{\psi}(\hat{\xi}_t|\mu_j) = \frac{\nabla\varphi(\hat{\xi}_t|\nu)}{|\omega^f_{\mu_j} - \hat{\xi}_t|^2}, \tag{16b}$$

where γ is positive constant. In Eq. (16), the 'repulsion' by the boundary is evaluated within the framework of the Hausdorff potential for each fixed point. Despite geometric singularity, the random sequence $\hat{\xi}_t$ successively covers the boundary points. In accordance with the $\hat{\xi}_t$-generation, the scheme dynamically updates the fixed points combined with the sequence $\hat{\xi}_t$ through the nondeterministic dynamics (14). This implies that the open space model ν can be adapted to smoothly varying scene. Such a stable adaptation process yields smooth control signal for practical vehicle mechanism maneuvering through the real world.

5 Experiments

The roadway model generation scheme was verified through experimental studies. Experimental results for an example scene are shown in Figs. 4 – 8. In these experiments, the initial guess of the fixed point set Ω^f is given as shown in Fig. 4; the vanishing point and left (right) width are allocated at center-top and left (right)-bottom of the scene image, respectively. A system of the Laplacian-Gaussian basin $\{\Lambda^{\mathfrak{G}}_i\}$ based on the initial guess is updated through the successive process (12) to yield statistical estimate of Ω^f as the steady state of the iteration. Resulted mapping set $\nu = \{\mu_i\}$ based

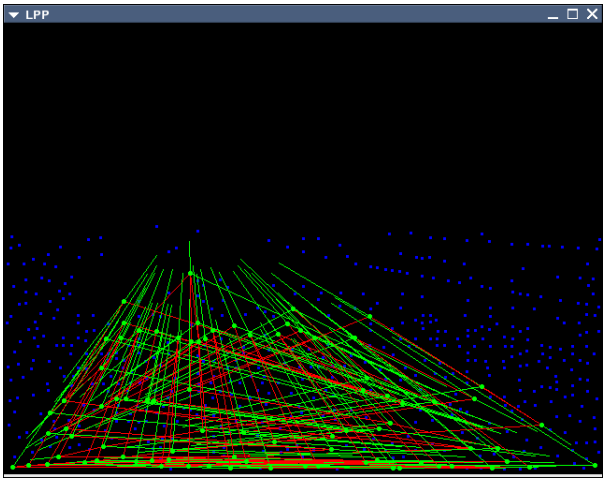

Figure 5: Computational Verification

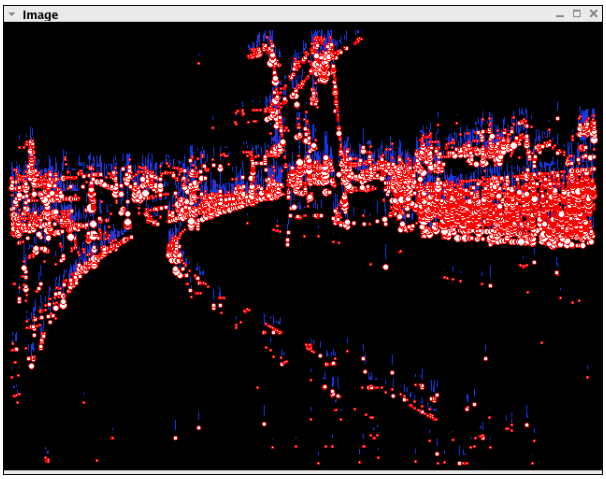

Figure 6: Break Down Image

on the fixed point estimate Ω^f is applied to visualize an estimate of the open space within the roadway area as shown in Fig. 4. The consistency of the mapping set ν is verified through the finite invariance test (8) as shown in fig. 5 where the invariant subset θ is visualized as the closed link on the local maxima $\tilde{\Theta}$. The existence of invariant subset Θ implies that a connected part of the open space in the scene is covered by the fractal attractor associated with the mapping set ν.

In the same scene, the break down pixels of the scale space model are detected as shown in Fig. 6 to relocate the boundaries as illustrated in Fig. 7, respectively. To relocate the boundaries, the random point $\hat{\xi}_t$ generated through the nondeterministic system (15) is matched with the break down pixels to evaluate the repulsion concentrated on the fixed points. By shifting the fixed points along the repulsion, the expansion of the attractor is confined within the obstacle free region. The consistency of the reduced attractor with the scale space model is verified via the finite invariance test, again, to yield the closed link as shown in Fig. 7 (a). In this figure, the effective part of the boundaries is specified in

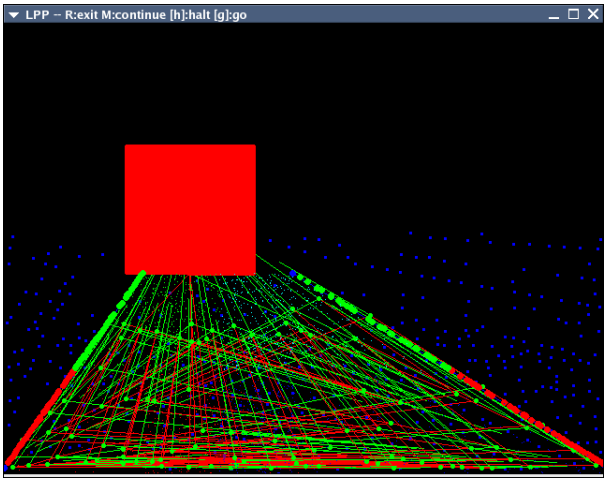

(a) Computational Verification

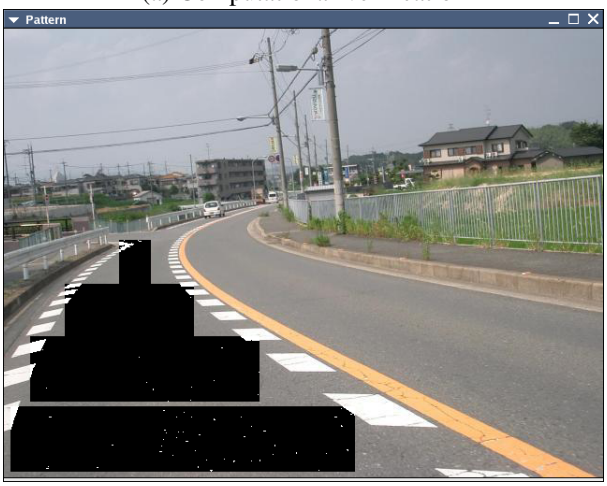

(b) Visualization

Figure 7: Model Refinement

terms of the nearest point $\lceil \xi \rceil$. The boundary estimate can be used to visualize break down free region directly as shown in Fig. 7 (b). In this refined area, IFS code ν is redesigned for *in-situ* adaptation of the roadway model as indicated in Fig. 8; re-designed mapping set ν is applied to the scene image for sampling the palette $\mathfrak{s}$ in refined roadway area. The connectedness of re-designed open space model is supported by the existence of invariant subset Θ with visualization on the scene image. Thus, fractal roadway model ν is fed back to the satellite image to extend the segment model $\check{\nu}$.

6 Concluding Remarks

Fractal dynamics is introduced on ineluctable randomness distributed in naturally complex scene. Based on anticipative information transferred via inter-viewpoint association, geometry of the maneuvering affordance is structuralized to design a fractal model for roadway pattern. Geometric disparity of designed model is evaluated in terms of Hausdorff potential for structurally consistent adaptation of the fractal code. The next step is stochastic design of maneuvering process cooperative with human's possible decisions.

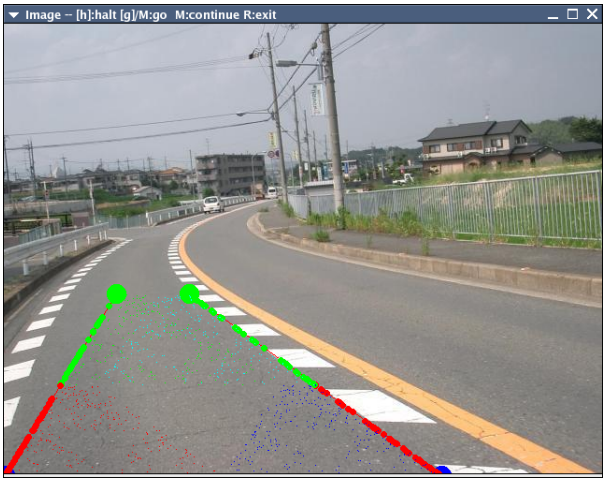

Figure 8: Road Following Process

References

[1] M. F. Barnsley. *Superfractals*, Cambridge University Press, 2006.

[2] Y. Chen and G. Medioni. Object modeling by registration of multiple range images. In *Proc. 1991 IEEE Int. Conf. Robotics and Automation*, pages III:2724–2729, 1991.

[3] P. W. Coppin, R. Pell, M. Wagner, J. R. Hayes, J.-L. Li, L. Hall, K. Fischer, D. Hirschfield, and W. Whittaker. EventScope: Amplifying human knowledge and experience via intelligent robotic systems and information interaction. In *Proc. IEEE-RoMan2000*, pages 292–296, 2000.

[4] M. Droske and M. Rumpf. Multiscale joint segmentation and registration of image morphology. *IEEE Trans. Pattern Anal. and Machine Intell.*, PAMI-29:2181–2194, 2007.

[5] T. Hamada and M. Fujie. Robotics for social safety. *Advanced Robotics*, 15:383–387, 2001.

[6] K. Kamejima. Laplacian-gaussian sub-correlation analysis for scale space imaging. *Int. J. Innov. Comp. Info. Con.*, 1:381–399, 2005.

[7] K. Kamejima. Image-based satellite-roadway-vehicle integration for informatic vicinity generation. In *Proc. IEEE-RoMan'06*, pages 334–339, 2006.

[8] K. Kamejima. Randomness-based scale-chromatic image analysis for interactive mapping on satellite-roadway-vehicle network. *J. Systemics, Cybernetics and Informatics*, 5:78–86, 2007.

[9] K. Kamejima. Chromatic information adaptation for complexity-based integration of multi-viewpoint imagery – a new approach to cooperative perception in naturally complex scene –. *Int. J. Innov. Comp. Info. Con.*, 4:109–126, 2008.

[10] D. G. Lowe. Object recognition from local scale-invariant features. In *Proc. Int. Conf. Computer Vision II*, pages 1150–1157, 1999.

[11] J. C. McCall and M. M. Trivedi. Driver behavior and situation aware brake assistance for intelligent vehicles. *Proc. IEEE*, 95:397–411, 2007.

[12] A. Parker. *In the Blink of an Eye*, The Free Press, 2003.

[13] Y. Zhao, L. Zhang, P. Li, and B. Huang. Classification of high spatial resolution imagery using improved gaussian markov random-field-based texture features. *IEEE Trans. Geosci. Remote Sens.*, GRS-45:1458–1468, 2007.